

# Comprehensive Characterization of Raw and Oxalic Acid Treated Ripen Cellulosic Biofiber from *Areca Catechu* Inflorescence as Substitute for Harmful Synthetic Products

Srinivas Arabilachi<sup>1,2</sup>, Sreenivasa Challakere Govindappa<sup>2</sup>, Bharath Kurki Nagaraj<sup>3,4</sup>, Brailson Mansingh Bright<sup>5</sup> and Joseph Selvi Binoj<sup>6,\*</sup>

<sup>1</sup>Department of Mechanical Engineering, Dr. T Thimmaiah Institute of Technology, KGF-563120, Visveswaraya Technological University - Belagavi, Karnataka, India

<sup>2</sup>Department of Mechanical Engineering, UBDT College of Engineering, Davangere-577004, Visveswaraya Technological University – Belagavi, Karnataka, India

<sup>3</sup>Department of Mechanical Engineering, GM Institute of Technology, Davangere-577006, Visveswaraya Technological University – Belagavi, Karnataka, India.

<sup>4</sup>Department of Engineering Design, GM University, Davangere-577006, Karnataka, India

<sup>5</sup>Department of Mechanical Engineering, Sri Ramakrishna Engineering College, Coimbatore - 641022, Tamilnadu, India

<sup>6</sup>Institute of Mechanical Engineering, Saveetha School of Engineering, Saveetha Institute of Medical and Technical Sciences (SIMATS), Saveetha University, Chennai-602105, Tamilnadu, India

**Abstract:** The inherent characteristics of natural fibers include a low density and a high strength-to-weight ratio, making them promising candidates for lightweight applications. The mechanical features of these strands are prejudiced by their chemical compositions and the cross-sectional area being the most variable factor affecting strength. In this research, strands were obtained by processing the ripen inflorescence of Areca tree and subjected to treatment with an oxalic acid ( $C_2H_2O_4$ ) solution to enhance their properties. The extracted fibers underwent examination for chemical, physical, mechanical, and morphological properties. The study findings indicate that fibers treated with a 4 wt.%  $C_2H_2O_4$  solution for 60 min exhibit superior properties. The strands segregated from the ripen inflorescence of areca tree treated with 4 wt.%  $C_2H_2O_4$  solution for 60 min exhibited a rise in cellulose proportion by 26.7%, tensile strength by 13.5%, crystallinity index by 16.6%, thermal endurance by 6.3% and appreciable surface roughness compared to the untreated fibers as viewed through Scanning Electron Microscope (SEM). The Fourier Transform Infrared (FTIR) analysis endorsed the observations of chemical analysis. The characterization of areca inflorescence fibers in this study highlights significant advantages for the advancement of composite materials.

**Keywords:** Oxalic acid treatment, Optimization, Pollution Management, Sustainability.

## HIGHLIGHTS

- Surface enhanced *Areca* inflorescence fiber (AIF) proposed for polymer composite reinforcement.
- High cellulose content (60.35 wt.%) noticed in 4 wt.% treated fiber by chemical composition test.
- Rough and porous nature of AIF promotes good bonding features with polymer matrix.
- High tensile strength (201.6 MPa) & low density ( $1.1 \text{ g/cm}^3$ ) reveals good mechanical properties.

- Measured CI value 57 % favors the drivable hydrophobic nature of AIF.

## INTRODUCTION

The current situation opens ample opportunities for reducing pollution in various production sectors. Consequently, natural fiber composites play a noteworthy role in mitigating environmental risks [1]. Natural fiber composites are biodegradable in nature, and because of their unique characteristics, such as good mechanical properties and manufacturing flexibility, raw material availability, low cost, and so on, they can be used for several applications, from aerospace to transportation packing substances [2,3]. They have found successful applications in various fields, especially in composite sectors. In spite of having minimal density compared to glass fiber in construction and engineering, they have been utilized

\*Address correspondence to this author at the Institute of Mechanical Engineering, Saveetha School of Engineering, Saveetha Institute of Medical and Technical Sciences (SIMATS), Saveetha University, Chennai - 602105, Tamilnadu, India; Tel: +91-8754379212; E-mail: binojlaxman@gmail.com

in textile, biosensors, biomedical, smart packaging, biopolymer and support structures [4]. In light of their excellent impact qualities, composites made from natural fibers are most appropriate for use in ballistics purposes. Using natural fibers can aid in addressing problems related to pollution, including issues like waste accumulation, landfill concerns, toxicity, and the emission of greenhouse gases. Since fibers made from plants are widely distributed throughout the environment, they are an affordable and sustainable resource [5,6]. The choice of natural fiber, still is contingent upon the particular demands of every purpose.

Natural fibers encompass plant fibers, animal fibers and mineral fibers. Cellulose and protein serve as the key constituents of plant and animal fibers, correspondingly. Moreover, the fiber plant can be categorized into stems, leaves, seeds, bark, xylem, and fruit [7]. These fibers are derivative of either meristematic tissue, a characteristic that varies depending on the species. Stem fibers, which encompass rice, corn stem, wheat, bamboo, and bagasse, are also part of this category. Fruit fibers consist of coconut and oil palm, while leaf fibers encompass pineapple, abaca, agave and sisal [8]. Examples of seed fibers are wider, cotton and kapok. Bark fibers include rosella, hibiscus, jute, abaca, ramie and soybean fiber [9]. Animal fibers consist of silk, wool, collagen fibers, bird fiber and hair. Mineral fibers, on the other hand, include asbestos, carbon, and glass [10,11]. Natural fibers have a few drawbacks when used as augmentation in polymer-based composite materials, in spite of all of its positives. They are incompatible with polymers used as substrates in the production of composite components, owing to its low wettability, and absorb a lot of moisture [12]. The incompatible properties of natural fiber with specific matrix materials poses a major obstacle to their use in particular fields [13,14]. Various methods such as chemical procedures, material coatings on natural fibers, and hybridization processes are employed to improve the mechanical and physical characteristics of the material. Before reinforcing natural fibers with polymeric composites, their compatibility can be enhanced by chemically treating their surface [15,16]. These chemical processes can decrease surface tension, cleanse the fiber's exterior, and strengthen the link among natural fibers and the polymeric matrix.

Anne et al. (2023) treated the fibers extracted from the roots of Zea Mays in 4 wt.% oxalic acid solution for 10 min to interrogate its influence on physio-

mechanical characteristics of the fiber [17]. Their observations portray that the treated Zea Mays root fibers exhibit comparatively rough surface with 23% increased tensile strength in relation to raw fibers. The fibers extracted from culms of *Bambusa blumeana* were pretreated by oxalic acid and treated with enzymes namely xylanase and pectinase at concentration of 300 U/mL and 250 U/mL correspondingly for further investigations by Michaela et al. (2023) [18]. Their experiments conclude that the treatments on fibers extracted from culms of *Bambusa blumeana* dissolved the wax content by 72 wt.% and enhanced the tenacity by 30% in comparison with the raw fiber. The treated fibers also had a tenacity range of 60 to 120 tex which suits well for textile applications. Oxalic acid treated natural fibers segregated from the log of *Lankaran acacia* was reinforced in polymer composites and tested for its physio-mechanical characteristics by Maguteeswaran et al. (2024) [19]. Their test results confirm that the composites with 20 wt.% treated fiber loading possessed maximum mechanical characteristics. They found that the tensile strength of the modified yarn loaded composites improved by 8.52% whereas the impact strength enhanced by 42.6% in comparison with the raw yarn armored composites.

Similar study was done by Vijay et al. (2023) on oxalic acid treated *Zanthoxylum acanthopodium* fibers reinforced polymer composites [20]. They also endorse that the composites with 20 wt.% treated fiber loading possessed maximum mechanical characteristics reporting a tensile strength of 47.3 MPa. Juvvi et al. (2021) characterized the oxalic acid modified natural strands segregated from the stem of *Symphirema involucreatum* for the possibility of usage as reinforcement material in polymer composites [21]. The *Symphirema involucreatum* stem fiber treated with 5 wt.% oxalic acid solution for 60 min exhibited cellulose content of 68.69 wt.% with tensile strength of 471.2 MPa having thermal stability upto 371 °C. Areca Catechu (betel palm), belongs to the Arecaceae family, was spread over 175,000 hectares in the nineteenth century, and has since grown to 4,97,000 hectares, representing a 65% growth in cultivation in India alone due to economic demand for harvested areca nuts. Bio leftovers created by it, on the other hand, are large enough to meet commercial demand [22,23]. The application of composites reinforced with areca/betel nut fibers offers significant benefits in the recent advancements of composite materials, particularly in areas such as electrical insulation applications [24]. Polymer reinforced with natural fiber composites are

also best suitable material for bullet proof and ballistic applications.

Even though several literatures report the characterization of areca fibers and its use as reinforcement in polymer composites, very few have reported the characterization areca inflorescence fibers [25-27]. Also, none have investigated the areca fibers subjected to surface modification with oxalic acid. Moreover, most of the researchers have used the fibers from dried areca inflorescence for their research whereas in the current work the fibers were extracted from ripen inflorescence [28]. The same fiber will have different physio-mechanical characteristics at different stages of growth and ripening which requires further investigation. Thus, the novelty of the current work lies in the surface treatment method followed and the stage at which the fiber is extracted from the areca inflorescence.

In order to boost and enhance sustainability, it is essential to take into account the physical, morphological, mechanical, chemical, and anatomical features of natural strands for their optimal and appropriate utilization [29]. It is noticed that different parts of areca plants having their own applications like, from sheath or leaves are used to produce bio plates by hot pressing and long fibers are extracted, trunk is used mainly for timber, decorative and furniture applications short fibers are extracted from areca husk. In this work effort made to extract fiber and characterization of areca inflorescence which is discarded after eradicating matured areca fruit from its bunch. The present work investigates the mechanical properties and characterization studies of the fibers extracted from a bio leftover Areca inflorescence (AI). After harvesting the betel nuts, the AI remains as bio leftover which is rich in fiber and left underutilized causing pollution and making bad fragrance to environment. This Areca inflorescence fiber (AIF) needs further investigation for possible utilization in composite industry. Especially the AIF need to withstand the polymerization temperature for reinforcement in polymer-based composites. The outer of the AIF desires to be coarse enough to get interacted and bond with the matrix on reinforcement. Moreover, AIF must have sufficient tensile strength to carry the loads transferred to it through the matrix in composite materials on reinforcement. For sixty minutes, the AIFs were exposed to varying oxalic acid ( $C_2H_2O_4$ ) ratios. This oxalic acid treated AIFs (OAIFs) were interrogated for its chemical, physical, mechanical and thermal properties to know the right concentration

of oxalic acid treatment which provides optimum characteristics to the fiber. This article presents the results of AIF and OAIF based on the tests conducted using techniques like FTIR, Scanning Electron Microscopy (SEM), Chemical Analysis, X-Ray Diffraction (XRD), Digital Scanning Calorimetry (DSC), and Thermo-Gravimetric Analysis (TGA).

## MATERIALS AND METHODS

### Materials

Areca inflorescence (AI) was obtained from the Dutishree areca farm in the Indian town of Arabilachi in the Bhadravathi taluk. Once matured, the raw AI collected as shown in Figure 1 is left to dry naturally in the sunlight for a period of 7 days [30]. Subsequently, the fibers are delicately loosened and freed from any foreign materials and outer layers through gentle smashing and water retting for 10 days [31]. Manual brushing is employed to extract the AIF strands carefully. The extracted AIFs are then submerged in water for a full day and subjected to multiple washing cycles to eliminate dust particles. Afterward, they are dehydrated in the daylight for 3 days to eliminate moistness [32]. Finally, the AIF is securely stored in an airtight bag for future processing. Oxalic acid powder was procured from M/s. Vasa Scientific Co. in, Bangalore, India which is analytical grade. The oxalic acid was used as such without any further purification process.

### Chemical Treatment of AIFs

AIFs undergo exposure to different concentrations of oxalic acid as shown in Figure 2. The fibers are soaked in solutions containing 1, 2, 3,4 and 5 wt.% concentration of oxalic acid for a duration of 60 min at room temperature, respectively [33]. To prepare these solutions, distilled water is utilized. Following the treatment, the OAIFs are thoroughly washed multiple times with distilled water [34]. They are then washed in distilled water until the pH reaches a neutral level and stored in an airtight bag for further characterization.

### Characterization of OAIFs

#### Chemical Study

The chemical compositions of AIF and OAIFs were explained using the standard techniques found in the literature, such as the Krusher–Hoffer method for cellulose, the Conrad method for wax, the Klason method for lignin, and the Standard NFT 12-008



**Figure 1:** Extraction of AIF (a) Young AI (b) Ripened AI (c) Collected left over AI (d) Drying of collected AI in sunlight (e) Sundried AI and (f) Extracted AIFs.



**Figure 2:** Oxalic acid treatment of AIFs (a) oxalic acid pellets and (b) oxalic acid treatment.

method for hemicellulose [35]. The AIF and OAIF ash content was reported in agreement with ASTM E1755-61 norm. Using the ASTM E1755-61 standard, the amount of moisture in the AIF and OAIFs was ascertained [36].

### **Physical and Mechanical Characteristics**

The density of AIF and OAIFs was determined using a pycnometer [37]. The diameter of fibers is found using optical micrometer with digital image capturing device [38]. 10 measurements were made to report the average diameter of the areca fibers. The tensile strength of AIF and OAIFs was determined using computerized INSTRON (5500R) universal

testing machine according to ASTM D3822 [39]. The specimens were prepared with a gauge length of 25 mm and fixed into grips. The test was conducted with cross head speed of 5 mm/min, 10 samplings are tested and average value was reported.

### **Surface Morphology**

Using a Hitachi (Model SU 3500) scanning electron microscope, the morphology of AIF and OAIFs was examined for surface alterations. Palladium-gold-encased specimens sputtered with electrons and photographs were taken at a 10 kV voltage [40]. SEM images were used along with image J software to measure the microfibril angle of the areca fibers.

### FTIR Studies

The AIF and OAIFs were ground into a fine powder using a grinder before conducting FTIR analysis. The powdered fibers were then compressed into pellets and inserted into a Shimadzu FTIR instrument. The samples were examined using a diamond cell attenuated total reflectance (ATR) mode. For each sample, a minimum of 64 scans ranging from 400 to 4500  $\text{cm}^{-1}$  were conducted [41]. Examining how the oxalic acid treatments affected the final spectra was the goal.

### XRD Studies

AIF and OAIFs were powder using a grinder for X-ray diffraction investigations. The powdered samples were held in a Teflon container. The examination was accomplished using a Bruker D8 Advanced Eco with Bragg-Brentano X-ray diffractometer. Concentrating geometry Cu-K irradiation at a wavelength of ( $\lambda = 1.54$ ) has been utilized for the measurement [42]. Diffraction intensity levels ranged from 10 to 80 degrees.

### TGA Studies

The thermal dilapidation of AIF and OAIFs was measured using a Shimadzu DTG 60 thermogravimetric analyzer. 10 mg of a powder mixture were heated in the analyzer at a rate of 10  $^{\circ}\text{C}/\text{min}$  from room temperature to 600  $^{\circ}\text{C}$  [43]. Using nitrogen flowing at a rate of 10 ml/min, the investigation was conducted in a  $\text{N}_2$  environment.

### DSC Studies

To analyze the thermodynamic response of AIF and OAIFs specimens at elevated temperatures, a Jupiter simultaneous differential scanning calorimeter (model STA 449 F3, M/s Netzsch Instruments Inc., Germany) connected to the Proteus program was utilized. To study the degradation process of a 10 mg pulverized AIF and OAIFs specimens, the temperature is increased in an alumina crucible in the presence of

nitrogen from room temperature to 450  $^{\circ}\text{C}$  at a rate of 10  $^{\circ}\text{C}/\text{min}$  in order to avoid oxidizing implications [44].

## RESULTS AND DISCUSSION

### Chemical Analysis of OAIFs

Table 1 lists the chemical makeup of AIF and OAIFs that have been oxalic acid-modified. Understanding the mechanical nature of yarns, which is directly influential to the mechanical features of bolstered composite, is made easier with the aid of information about the chemical proportion of the strands that is acquired by chemical examination [45]. In contrast with various oxalic acid-modified OAIFs modified with 1, 2, 3, and 5 wt.% concentration, it is observed that the weight percentage of cellulose is highest for OAIF modified with 4 wt.%  $\text{C}_2\text{H}_2\text{O}_4$  concentration. Furthermore, it has been shown that when the concentration of the oxalic acid modification in OAIFs is increased, the weight percentage of the amorphous portions such as hemicellulose, lignin, and wax continuously decreased. This is caused by the OAIF's amorphous components being continuously removed as the concentration of the oxalic acid modification increases [46]. The oxalic acid disintegrates the amorphous contents of the areca fibers through acid hydrolysis. Since OAIFs are exposed to an oxalic acid solution of higher concentration, their cellulose deteriorates, which causes the cellulose weight percentage to drop for OAIFs modified with 5 wt.%  $\text{C}_2\text{H}_2\text{O}_4$  concentration. In general, the mechanical, thermal, and crystalline attributes of a fiber are maximized when its cellulose content is higher in weight percentage. Therefore, the OAIFs that were exposed to  $\text{C}_2\text{H}_2\text{O}_4$  concentration of 4 wt.% are the ones that were optimally oxalic acid modified.

Table 2 compares the chemical content of AIF and OAIF with 4 wt.% oxalic acid treatment with various untreated and modified naturally occurring fibers that

**Table 1: Chemical Composition of AIF and OAIFs**

Fiber	Cellulose (wt.%)	Hemicellulose (wt.%)	Lignin (wt.%)	Wax (wt.%)	Ash (wt.%)	Moisture (wt.%)
AIF	47.61	18.55	22.61	0.29	1.7	9.24
OAIF (1 wt.%)	52.62	14.48	21.54	0.28	2.54	8.54
OAIF (2 wt.%)	54.57	13.93	20.57	0.28	3.53	7.12
OAIF (3 wt.%)	57.56	10.62	18.71	0.27	4.87	7.97
OAIF (4 wt.%)	60.35	9.28	17.12	0.26	6.01	6.98
OAIF (5 wt.%)	59.45	9.21	17.11	0.26	7.2	6.77

**Table 2: Comparison of Chemical Composition of AIF and OAIF with other Fibers**

Fiber	Cellulose (wt.%)	Hemicellulose (wt.%)	Lignin (wt.%)	Wax (wt.%)	Ash (wt.%)	Moisture (wt.%)	Ref
AIF	47.61	18.55	22.61	0.29	1.7	9.24	Present
OAIF (4 wt.%)	60.35	9.28	17.12	0.26	6.01	6.98	
Areca palm leaf stalk	57.49	18.34	7.26	0.71	1.43	9.35	[45]
Treated Areca palm leaf stalk (5 wt.%)	68.54	6.13	5.87	0.32	1.10	3.62	
Cyrtostachys renda	45.15	22.88	18.77	-	-	-	[47]
Treated Cyrtostachys renda (5 wt.%)	47.31	19.68	18.46	-	-	-	
Cannonball	69.23	14.98	14.25	0.78	3.25	8.96	[48]
Treated Cannonball (4 wt.%)	72.19	11.23	12.90	0.56	5.97	8.89	
Aerial roots of banyan tree	67.32	13.46	15.62	0.81	3.96	10.21	[49]
Treated aerial roots of banyan tree	70.4	10.74	12.7	0.69	5.86	9.91	
Licuala grandis leaf sheath	49.13	11.75	26.15	0.31	1.62	11.05	[50]
Treated Licuala grandis leaf sheath	56.92	7.74	24.50	0.10	2.00	8.75	
Cocos nucifera L. peduncle	50.11	11.98	24.90	0.31	1.6	11.1	[51]
Treated Cocos nucifera L. peduncle	56.78	9.86	20.59	0.21	3.85	8.71	

were isolated from plants. In contrast to AIF, which displays 47.61 wt% of cellulose, OAIF with 4 wt.% oxalic acid treatment has 60.35 wt% proportion of cellulose. On the contrary, hemicellulose reduced from 18.55 wt.% for AIF to 9.28 wt.% for OAIF with 4 wt.% oxalic acid treatment. Several researchers noticed a similar pattern in the recovered and modified plant fibers, with a rise in cellulose weight percentage and a reduction in hemicellulose weight percentage [52]. As a result, the oxalic acid bleaching of AIF also caused a drop in wax, lignin, and moisture weight percentage. Improved matrices binding properties are made possible in composites with polymer matrix augmented with OAIF with 4 wt.% oxalic acid treatment due to the elimination of wax and lignin components. The OAIF with 4 wt.% oxalic acid treatment's increased weight percentage of ash proportion indicates that the cellulose proportion of the fibers has improved.

### Physico-Mechanical Analysis

The separation process, chemical makeup, and surface modifications applied to the plant fibers all affect their ability to withstand stress. Table 3 displays the physico-mechanical characteristics of AIF and OAIFs, along with a comparison to various plant-based fibers. The tensile strength of the OAIF was found to rise strength of 201.6 MPa, which is 13.5% greater

than AIF. OAIF with 4 wt.% oxalic acid treatment's improved tensile properties can be attributed to its greater cellulose weight percentage [53]. The sudden failure after the ultimate tensile strength explains the fragility of both AIF and OAIFs. While OAIF with 4 wt.% oxalic acid treatment's extension at break was 19.5% less than AIF, it had a young's modulus of 7.1 GPa, that is 20.3% greater than AIF. The stress-strain plot of AIF and OAIFs were shown in Figure 4. Following an oxalic acid treatment procedure, it was discovered that the density of OAIF with 4 wt.% oxalic acid treatment increased by 1.26% as a result of the fiber's amorphous components being removed and the pores being compactly filled. In the case of OAIF with 4 wt.% oxalic acid treatment augmented in matrix, the rise in density would be extremely small, adequate to yield composites with better specific strength, low weight, and also the density was comparable to that of the remaining natural fibers shown in Table 3. In comparison to AIF, which has a diameter of 416.5  $\mu\text{m}$ , OAIF with 4 wt.% oxalic acid treatment, with a measurement of 401  $\mu\text{m}$ , has a smaller diameter (Figure 3). The elimination of water content and non-crystalline components caused OAIFs to decrease in size [54]. The OAIFs with low microfibril angle enhance the mechanical characteristics of the polymer composites when reinforced. The weakening in

**Table 3: Physical and Mechanical Parameters of AIF and OAIF**

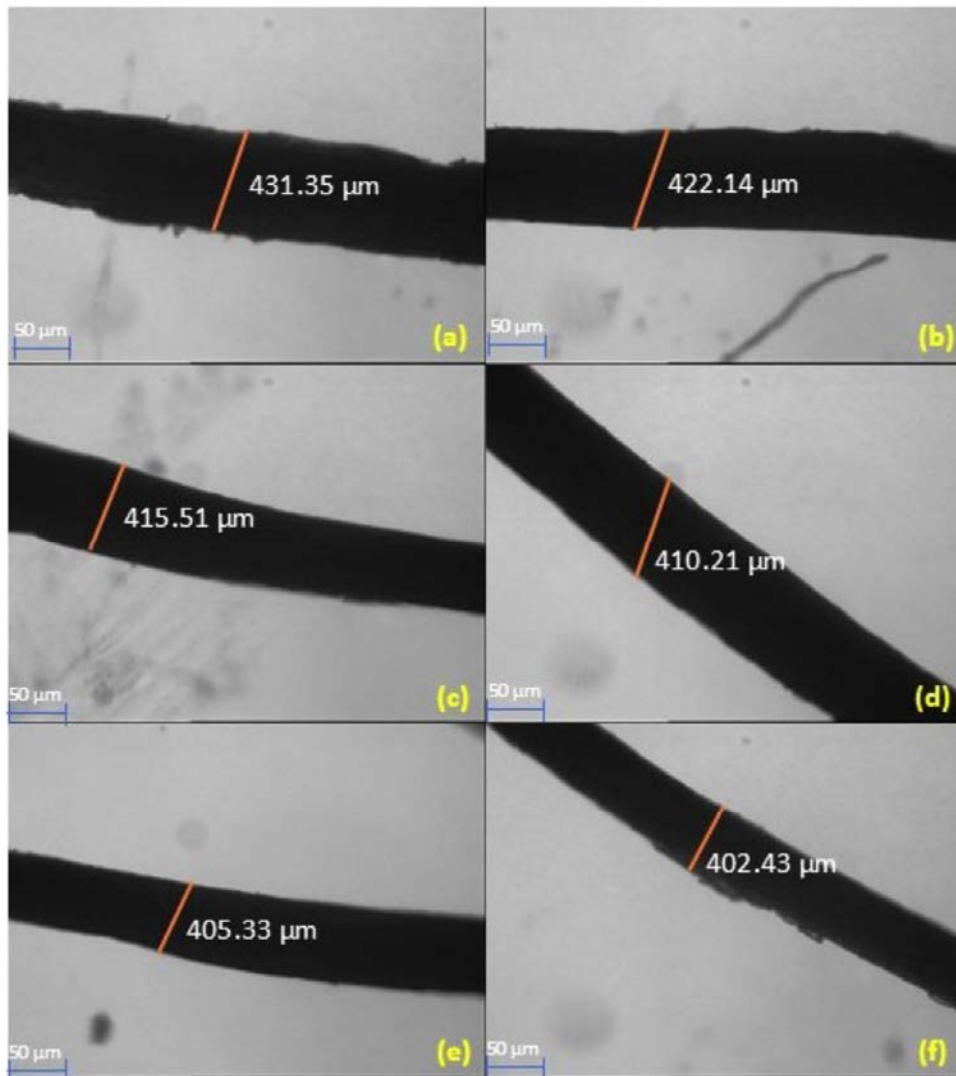
Fiber	Physical properties		Mechanical properties				Ref
	Diameter ( $\mu\text{m}$ )	Density ( $\text{kg/m}^3$ )	Tensile strength (MPa)	Young's Modulus (GPa)	Elongation at Break (%)	Microfibril Angle ( $^\circ$ )	
AIF	416.5 $\pm$ 21.63	1094	177.6 $\pm$ 18.37	5.9 $\pm$ 0.71	9.2 $\pm$ 0.76	6.73 $\pm$ 0.33	Present*
OAIF (1 wt.%)	409.2 $\pm$ 20.34	1097	186.2 $\pm$ 18.92	6.4 $\pm$ 0.78	8.6 $\pm$ 0.71	6.38 $\pm$ 0.32	
OAIF (2 wt.%)	406.8 $\pm$ 20.29	1102	192.8 $\pm$ 19.61	6.7 $\pm$ 0.83	8.2 $\pm$ 0.69	5.92 $\pm$ 0.32	
OAIF (3 wt.%)	403.6 $\pm$ 19.82	1105	197.3 $\pm$ 20.01	6.9 $\pm$ 0.87	7.7 $\pm$ 0.68	5.61 $\pm$ 0.31	
OAIF (4 wt.%)	401.7 $\pm$ 19.3	1108	201.6 $\pm$ 21.27	7.1 $\pm$ 0.97	7.4 $\pm$ 0.63	5.34 $\pm$ 0.28	
OAIF (5 wt.%)	399.4 $\pm$ 18.91	1110	203.7 $\pm$ 22.18	7.2 $\pm$ 0.98	7.1 $\pm$ 0.62	5.18 $\pm$ 0.28	
Areca palm leaf stalk	330 $\pm$ 17.9	1090	334.66 $\pm$ 21.46	7.64 $\pm$ 1.13	4.38 $\pm$ 1.15	-	[45]
Treated Areca palm leaf stalk (5 wt.%)	314 $\pm$ 16.2	1170	486.41 $\pm$ 35.57	9.89 $\pm$ 1.46	4.91 $\pm$ 1.82	-	
Aerial roots of banyan tree	0.09–0.14	1234	19.37 $\pm$ 7.72	1.8 $\pm$ 0.40	1.8 $\pm$ 0.40	10.88 $\pm$ 1.19	[49]
Treated aerial roots of banyan tree (5 wt.%)	0.08–0.12	1269	20.45 $\pm$ 12.20	0.82 $\pm$ 0.32	1.6 $\pm$ 0.50	10.17 $\pm$ 1.58	
Cannonball Fibers	69.97–75.94	1049	42.2 $\pm$ 10.5	2.1 $\pm$ 0.789	4.6 $\pm$ 0.63	17.23 $\pm$ 1.78	[48]
Treated Cannonball Fibers (4 wt.%)	47.11–54.96	1091	71.5 $\pm$ 25	4.15 $\pm$ 1.572	4.1 $\pm$ 13.54	16.27 $\pm$ 1.01	
Licuala grandis leaf sheath	139.87 $\pm$ 23.02	1245	140.8 $\pm$ 38	3.82 $\pm$ 0.7	3.27 $\pm$ 0.9	5.98 $\pm$ 0.26	[50]
Treated Licuala grandis leaf sheath	130.18 $\pm$ 19.21	1263	159.4 $\pm$ 41	4.73 $\pm$ 1.2	3.12 $\pm$ 0.6	5.11 $\pm$ 0.21	
Cocos nucifera L. peduncle	543.4 $\pm$ 22.7	1258	184.6 $\pm$ 18.34	5.5 $\pm$ 0.7	7.6 $\pm$ 0.6	6.36 $\pm$ 0.32	[51]
Treated Cocos nucifera L. peduncle	429.4 $\pm$ 20.5	1269	206.3 $\pm$ 21.64	6.7 $\pm$ 0.8	6.7 $\pm$ 0.5	5.21 $\pm$ 0.26	

mechanical features of the OAIF with 5 wt.% oxalic acid treatment is due to the damage caused to OAIF due to excess concentration of oxalic acid.

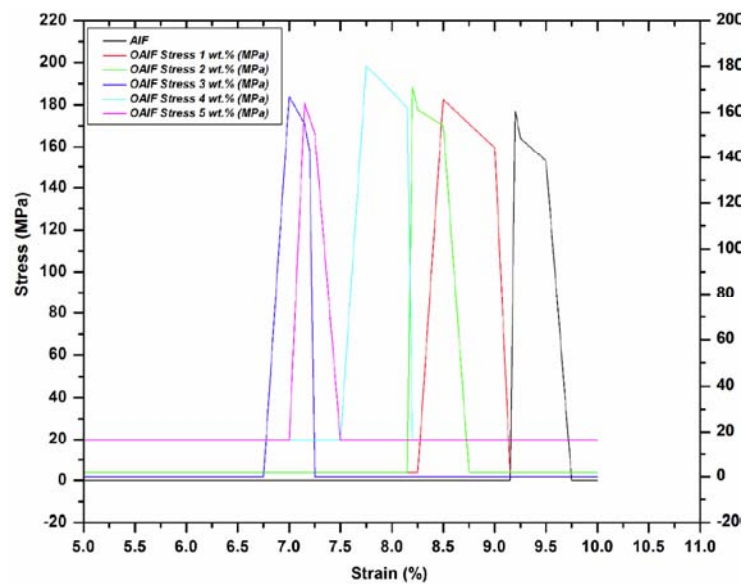
### Surface Morphology

Figure 5 illustrate the surface morphology of AIF and OAIFs. Figure 5a-f demonstrates the alterations in the surface of OAIFs after different treatment percentages of  $\text{C}_2\text{H}_2\text{O}_4$ . The findings reveal an

increase in surface roughness with rising  $\text{C}_2\text{H}_2\text{O}_4$  concentrations. The AIF's outer surface is observed to be filled with non-cellulosic compounds and pectin which binds fibrils throughout the exterior of the fiber as shown in Figure 5a [55]. These non-cellulosic compounds are loosely bound to the AIF's surface which makes the exterior of the fiber oily and smooth in nature. The fibrous structure is also slightly visible on the surface of the AIF longitudinally parallel to the axis of the fiber owing to its cellulose content [56].



**Figure 3:** Diameter measurement of (a) AIF, (b) OAIF (1 wt.%), (c) OAIF (2 wt.%), (d) OAIF (3 wt.%), (e) OAIF (4 wt.%) and (f) OAIF (5 wt.%).



**Figure 4:** Stress-strain plot of AIF and OAIFs.

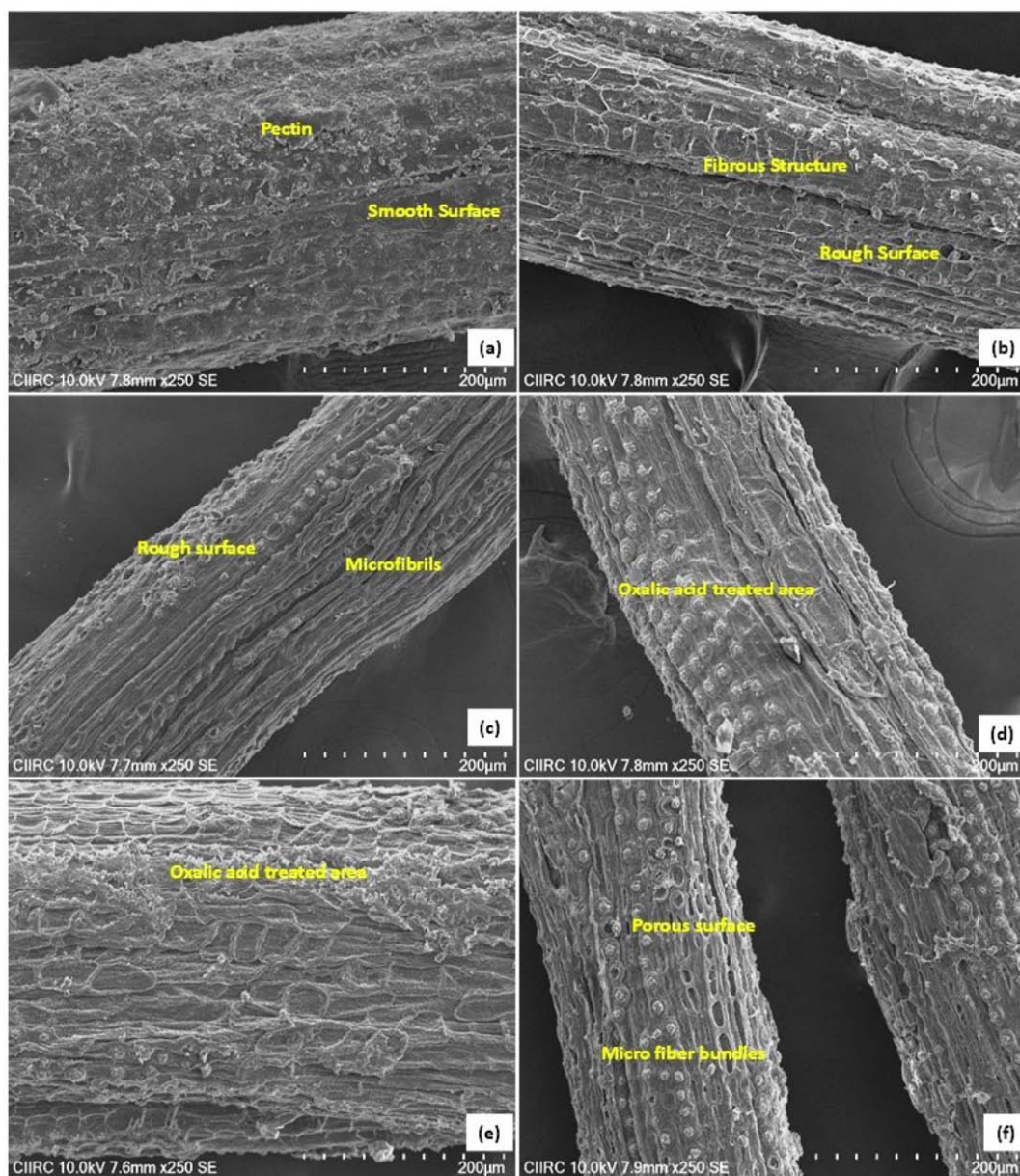


**Figure 5:** Morphological studies of AIF (a) AIF, (b) OAIF (1 wt.%), (c) OAIF (2 wt.%), (d) OAIF (3 wt.%), (e) OAIF (4 wt.%) and (f) OAIF (5 wt.%).

This structural integrity of AIF is not conducive to create better physical bonding with the matrix when reinforced in polymer composites. After treatment with  $C_2H_2O_4$ , the surface of OAIFs becomes rougher as shown in Figure 5b and c, facilitating better bonding with reinforcement and reducing the likelihood of fiber pullouts with the matrix. The  $C_2H_2O_4$  treatment even exposes the OAIF's cellulose content with micro fiber bundles as seen in Figure 5d-f leading to better interaction with the matrix. This can be attributed to the elimination of non-cellulosic materials and dirt from the OAIF throughout the oxalic acid modification procedure [57]. In polymeric matrix composite materials, these OAIFs with rough exteriors that are reinforced show

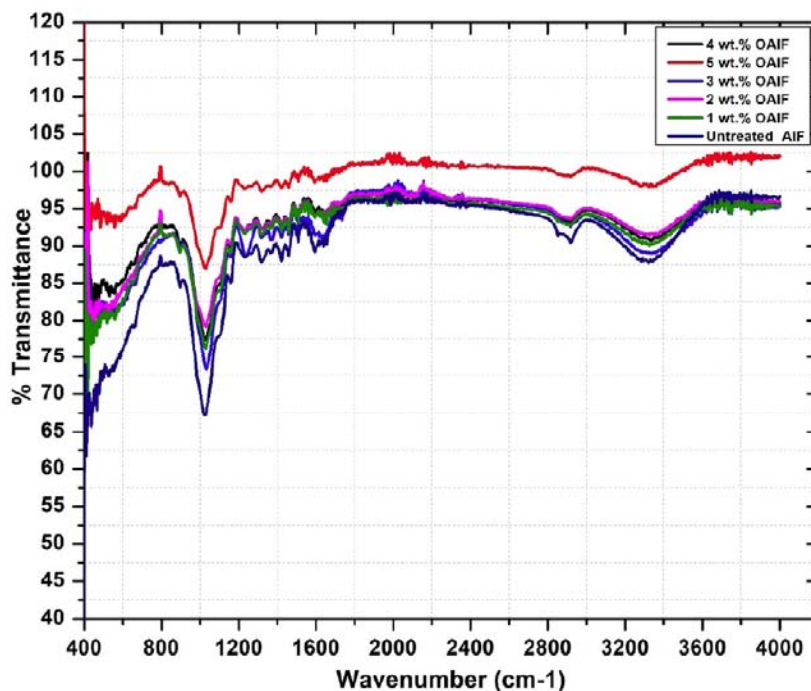
improved interfacial bonding among the base material and the fiber, which improves the mechanical characteristics of the resultant composite.

### FTIR Analysis

Fluctuations in the spectra graph obtained through FTIR analysis in Figure 6 highlights the alterations in the composition of AIF under various surface modification treatments. The discernible troughs in the graphs further listed in Table 4 serve as evidence of the presence of distinct chemical bonds, aiding in the identification of cellulose, hemicellulose, and lignin. Noteworthy troughs are discernible at  $3363\text{ cm}^{-1}$ ,  $2946\text{ cm}^{-1}$ ,  $1608\text{ cm}^{-1}$ ,  $1407\text{ cm}^{-1}$ ,  $1213\text{ cm}^{-1}$ , and  $1004\text{ cm}^{-1}$ ,

**Table 4: Peak Positions in FTIR Spectra of OAIFs**

Peak position based on wavenumber (cm <sup>-1</sup> )	Related functional group	Reference
3363	O-H vibrations of cellulose	[58]
2946	C-H vibrations of cellulose	[59]
1608	C-O stretching of hemicellulose	[62]
1407	-CO bending of lignin	[60]
1213	-CH stretching of acetyl group	[61]
1004	C=C bending of $\beta$ -glucosidic acid	[48]

**Figure 6:** FTIR spectra of AIF and OAIFs.

indicative of the presence of cellulose, moisture particles, wax, hemicellulose, and lignin characterized by O-H, C-H, C-O, -CO, -CH, and C=C bonds and acetyl group [58,59]. Specifically, the trough at 3363 cm<sup>-1</sup> correspond to O-H and bond, revealing the occurrence of cellulose. This trough becomes more pronounced after post-treatments in OAIFs, signifying an increased cellulosic content achieved by the removal of external impurities. The existence of wax is designated by the valley at 2946 cm<sup>-1</sup> in the obtained spectra (Fan *et al.* 2024). The two additional troughs at 1608 cm<sup>-1</sup> and 1407 cm<sup>-1</sup> are credited to C-O and C-C bonds, which represent hemicellulose and lignin. These troughs gradually diminish with the escalation of concentration of C<sub>2</sub>H<sub>2</sub>O<sub>4</sub> treatment in OAIFs, suggesting that chemical treatments partially eliminate hemicellulose and lignin from the OAIF [60]. The valley visible at 1213 cm<sup>-1</sup> demonstrates the occurrence of

acetyl group in the AIF and OAIF. The trough at 1004 cm<sup>-1</sup> designates the occurrence of  $\beta$ -glucosidic acid in the AIF and OAIF [61]. The partial elimination of amorphous components from the OAIF as a result of the oxalic acid modification is supported by the FTIR examination.

### XRD Analysis

Figure 7 presents the XRD plot of AIF and OAIFs. In the current study, AIF and OAIFs display two prominent peaks at  $2\theta$  of 16.4° and 22.2°. The peak observed at 22.2° exhibits sharpness and high intensity, signifying the presence of crystalline cellulose on the (0 0 2) crystallographic plane [63]. Conversely, the secondary peak at 16.4° corresponds to the (1 0 -1) crystallographic plane, representing the occurrence of amorphous components such as amorphous hemicellulose, lignin, wax and pectin. The presence of

cellulose quality is indicated by peaks in XRD graphs, and this can be substantiated through the calculation of Crystalline Index (CI) and Crystallite Size (CS) [64] using the formulas (1) & (2) below and listed in Table 5.

$$CI = (I_{22}-I_{16})/I_{22} \quad (1)$$

where  $I_{22}$  is the maximum intensity of crystalline peak at  $2\theta = 22.2^\circ$  and  $I_{16}$  is the intensity of amorphous peak at  $2\theta = 16.4^\circ$ .

$$CS = K\lambda\beta\cos\theta \quad (2)$$

where,  $K = 0.89$  is Scherrer's constant,  $\lambda$  is the wave length of the radiation,  $\beta$  is the peak's full-width at half-maximum (FWHM) and  $\theta$  is the Bragg's diffraction angle.

It is evident that the CI increases by 4.1, 10.4, 14.5, 18.7 and 16.6 percent for OAIF (1 wt.%), OAIF (2 wt.%), OAIF (3 wt.%), OAIF (4 wt.%) and OAIF (5 wt.%) respectively compared to AIF, achieved by the removal of amorphous hemicellulose, lignin, wax and pectin. The OAIF's (5 wt.%) improved mechanical and physical properties as well as compact nature make it a more effective strengthening substance for polymeric composites, as seen by its maximum CI value [65]. The decline in hydrophilic character of the OAIFs is revealed by a rise in quantitative value of CS compared to AIF following the oxalic acid treatment.

## TGA Analysis

The thermal dilapidation characteristics of natural fibers rely on the levels of cellulose, hemicellulose, and lignin present. Oxalic acid treatments chemically modify the fiber surface, eliminating unstable impurities and improving thermal properties. Figure 8 displays the AIF and OAIF's TGA-DTG plots, which show their thermal endurance. The AIF and OAIFs were subjected to a thermal test involving heating from room temperature to  $600^\circ\text{C}$ . The variation in mass across this temperature range shown in Table 6 provides insights into their stability amid temperature fluctuations. The specimens were heated above room temperature, and it was noted that moisture particles were evaporating up to  $113^\circ\text{C}$  [66]. AIF and OAIFs show a slight weight decrease as a result of moisture evaporation. OAIFs have lost fewer mass since the amount of moisture has decreased as a result of the oxalic acid modification. The cellulose, glycosidic bonds of hemicellulose and lignin gets depolymerized in the temperature range of  $236^\circ\text{C}$  to  $287^\circ\text{C}$  for AIF and OAIFs. Lesser weight loss is noticed for OAIFs especially OAIF (4 wt.%) owing to the OAIF's amorphous constituents, such as hemicellulose and lignin, have been partially removed [67].

The notable decrease in mass in the temperature span from  $288^\circ\text{C}$  to  $377^\circ\text{C}$  is indicative of the cellulose disintegration in AIF and OAIFs. The rest of the

**Table 5: CI and CS of AIF and OAIFs**

Fiber	Crystalline index (CI) (%)	Crystallite Size (CS) (nm)	Reference
AIF	48	12.6	Present study
OAIF (1 wt.%)	50	13.3	
OAIF (2 wt.%)	53	13.9	
OAIF (3 wt.%)	55	14.4	
OAIF (4 wt.%)	57	14.8	
OAIF (5 wt.%)	56	14.9	
Licuala grandis leaf sheath	48	1.26	[50]
Treated Licuala grandis leaf sheath	54	1.73	[49]
Aerial roots of banyan tree	72.47	6.28	
Treated aerial roots of banyan tree (5 wt.%)	76.35	7.74	[48]
Cannonball Fibers	65.29	26.73	
Treated Cannonball Fibers (4 wt.%)	72.73	32.39	[47]
Cyrtostachys renda	50	-	
Treated Cyrtostachys renda (5 wt.%)	56	-	[51]
Cocos nucifera L. peduncle	50	14.6	
Treated Cocos nucifera L. peduncle	54	13.1	

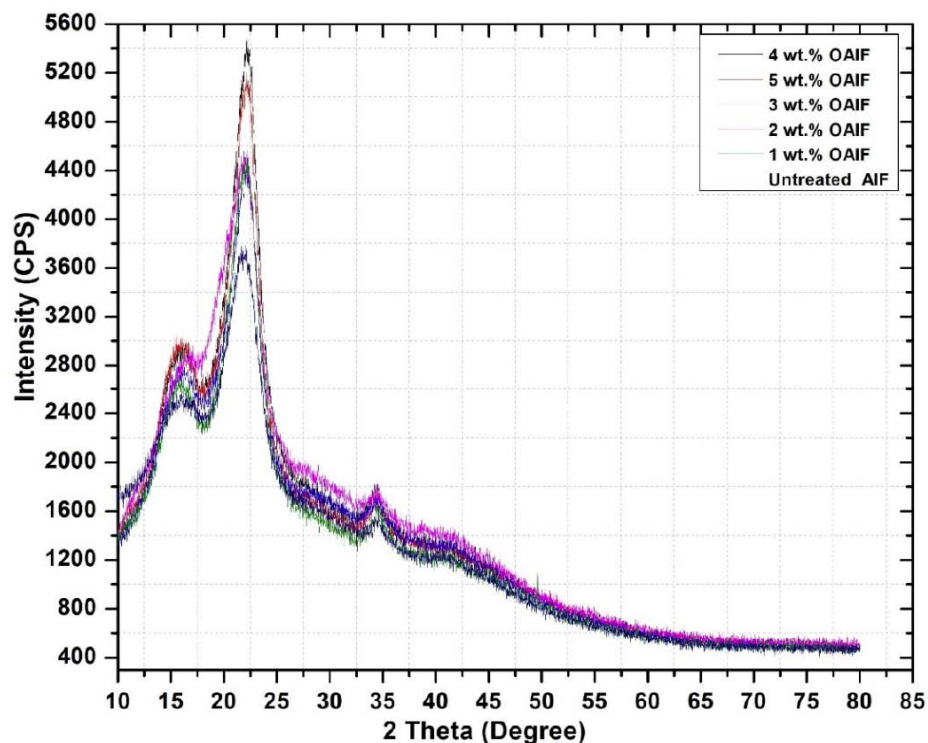


Figure 7: XRD spectra of AIF and OAIFs.

reduction in weight for AIF and OAIFs that was seen above 378°C can be attributed to the partial lignin and wax disintegration [68]. The alteration of the crystal configuration in OAIFs due to oxalic acid modification is the reason for the reduction in residual char at 600°C when weighed against AIF. Understanding the fiber's composition, thermal stability, and degrading behavior is essential for their successful usage in a variety of applications, including polymer composites. This is made possible by the inflection point in the DTG curve. Researchers and engineers can more accurately forecast how natural fibers will behave under processing and end-use settings by examining the location and characteristics of the inflection point, guaranteeing maximum performance and longevity [69]. The DTG curve disparity depicts an inflection point for the fibers AIF, OAIF (1 wt.%), OAIF (2 wt.%), OAIF (3 wt.%), OAIF (4 wt.%) and OAIF (5 wt.%), accordingly, at around 327°C, 339°C, 341°C, 343°C, 348°C, and 346°C, suggesting an elevation in the deteriorating event to greater temperatures. In comparison to AIF, OAIFs have superior thermal stability, as seen by the significantly smaller weight loss seen in each deterioration stage. Table 7 lists the char residue of AIF and OAIFs in comparison with other raw and treated natural fibers. AIF, OAIF (1 wt.%), OAIF (2 wt.%), OAIF (3 wt.%), OAIF (4 wt.%) and OAIF (5 wt.%) have kinetic activation energies ( $E_a$ ) of 66.9 kJ/mol, 68.4 kJ/mol, 69.9 kJ/mol, 70.7 kJ/mol, 71.6

kJ/mol and 71.2 kJ/mol, correspondingly, according to Broido's equation (3) [70]. The estimated  $E_a$  levels are greater than the 60 kJ/mol energy required to start the decomposition of wood.

$$\ln(\ln(1/y)) = -(E_a/R)((1/T) + K) \quad (3)$$

Where  $R$  (8.32 J/mol K) is the Universal Gas constant,  $w_t$  is the Mass of the sample at any time  $t$  and  $w_0$  - Initial mass of the sample,  $T$  is the Temperature in K,  $y$  is the Normalized weight ( $w_t/w_0$ ).

Table 6: Weight Loss Percentage of AIF and OAIFs

Temperature range (°C)	28-113	236-287	288-377
AIF	8.1	17.4	49
OAIF (1 wt.%)	7.8	16.9	47
OAIF (2 wt.%)	7.5	16.1	46
OAIF (3 wt.%)	7.1	15.4	44
OAIF (4 wt.%)	6.7	14.3	42
OAIF (5 wt.%)	6.5	14.8	43

### DSC Analysis

The DSC contour for AIF and OAIFs are shown in Figure 9. Both The AIF and OAIFs were found to have an endothermic peak, roughly ranging from 34°C to

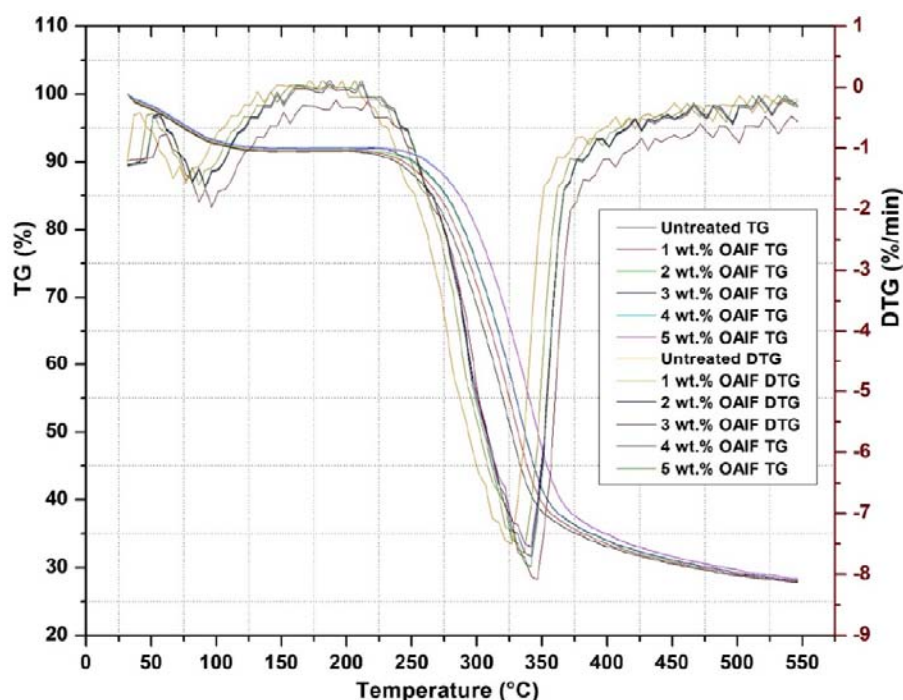


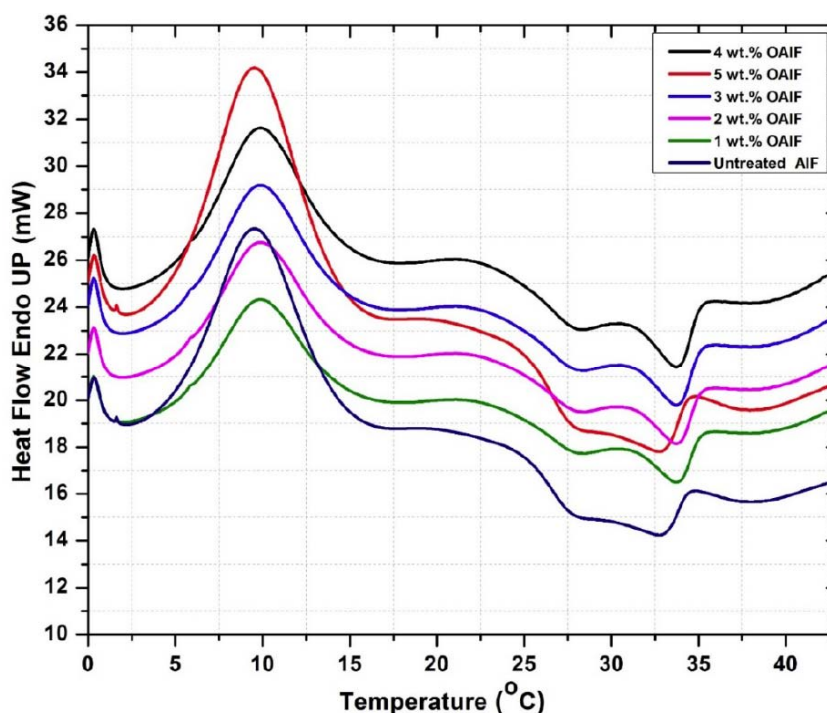
Figure 8: TGA spectra of AIF and OAIFs.

Table 7: Char Residue of AIF and OAIFs

Fibers	Char residue (wt.%)	Reference
AIF	22.02	Present study
OAIF (1 wt.%)	22.37	
OAIF (2 wt.%)	22.63	
OAIF (3 wt.%)	22.89	
OAIF (4 wt.%)	23.15	
OAIF (5 wt.%)	23.01	
Areca palm leaf stalk	0.82	[45]
Treated Areca palm leaf stalk (5 wt.%)	1.45	
Aerial roots of banyan tree	22.31	[49]
Treated aerial roots of banyan tree (5 wt.%)	18.67	
Cannonball Fibers	23.7	[48]
Treated Cannonball Fibers (4 wt.%)	26.8	
Cyrtostachys renda	11.41	[47]
Treated Cyrtostachys renda (5 wt.%)	25.07	
Licuala grandis leaf sheath	31.19	[50]
Treated Licuala grandis leaf sheath	33.02	

148°C, indicating the amount of energy needed to dry the fibers [71]. As a result of the lignin and hemicellulose in the AIF and OAIFs depolymerizing, an exothermic spike is detected in the temperature spectrum of 149°C to 219°C. OAIFs has a lower peak's

magnitude, broadness, and deep than AIF since the fiber's lignin and hemicellulose were partially removed during the oxalic acid modification procedure. The subsequent endothermic spike observed within the temperature spectrum of 220°C to 322°C is linked to



**Figure 9:** DSC spectra of AIF and OAIFs.

the cellulose breakdown that occurs in the AIF and OAIFs [72]. The final exothermic spike in the temperature spectrum ranging from 321°C to 372°C is indicative of the partial lignin and wax breakdown in AIF and OAIFs. Owing to the lignin and wax dissolving from the yarn through the oxalic acid treatment procedure, this spike is weaker for OAIFs than AIF. Wax and lignin in the strands volatilize when the DSC plot fluctuates further than 373°C [73,74]. Upon analyzing the whole procedure, it was found that the OAIFs required more energy to deteriorate than the AIF, showing an enhancement in the thermal endurance of the OAIFs due to the oxalic acid modification procedure.

## CONCLUSION

The fibers were obtained from the areca tree's ripen inflorescence post-harvesting of nuts. Subsequently, the fibers were subjected to treatment with  $C_2H_2O_4$  at different concentrations, specifically 1 wt.%, 2 wt.%, 3 wt.%, 4 wt.% and 5 wt.%. Following this treatment, various characterizations, including morphological, physical, chemical, XRD, FTIR, TGA, and DSC, were conducted. The results were obtained, leading to the following conclusions.

- Characteristics of fibers are influenced by the existence of cellulose. It has been clearly proven that cellulose percentage experiences a

noticeable enhancement with OAIF (4 wt.%) having maximum value of 60.34 wt.% which is further endorsed by FTIR analysis.

- Surface morphologies of OAIF (4 wt.%) display improved wettability by eliminating the outer layer of lignin, wax, and loosened impurities, resulting in a rough texture compared to other OAIFs and AIF. However, excessive oxalic acid treatment at 5 wt.% removes the linkages between outer cells, noticeably weakening the OAIF (5 wt.%).
- Tensile strength of OAIFs is improved by enhancing the cellulose and removing the amorphous content with OAIF (4 wt.%) having the maximum value of  $201.6 \pm 21.27$  MPa and modulus  $7.1 \pm 0.97$  GPa. Interestingly, OAIF (4 wt.%) exhibit superior strength compared to those treated with 5 wt.%. This is attributed to an excessive reaction that weakens the fibers in the latter case.
- Chemical modification boosts the crystalline properties of OAIFs, as clearly confirmed by XRD analyses. The CI of OAIF (4 wt.%) increased by 18.7% compared to AIF.
- The resulting enhancement in thermal stability for OAIFs was substantiated through TGA and

DSC analyses. The TGA analysis reveals the thermal stability of OAIF (4 wt.%) to be 236 °C.

As a result, it is affirmed that OAIFs exhibit considerable proficiency and have the potential to substitute conventional synthetic fibers in diverse applications in industries requiring lightweight polymer composites. Further optimizations can be done using machine learning techniques on the parameters like oxalic acid concentration, treatment duration and treatment temperature to identify the specific application of the OAIFs.

## ETHICS APPROVAL AND CONSENT TO PARTICIPATE

All the authors demonstrate that they have adhered to the accepted ethical standards of a genuine research study. Also, individual consent from all the authors was undertaken to publish the data prior submitting to journal.

## CONSENT FOR PUBLICATION

Written formal consent ensures that the publisher has the author's permission to publish research findings.

## AVAILABILITY OF DATA AND MATERIALS

This is an ongoing research work and hence the data cannot be shared at this moment.

## COMPETING INTERESTS

No potential conflict of interest was reported by the authors.

## FUNDING

No funding was received for this work.

## ACKNOWLEDGEMENTS

Not applicable.

## REFERENCES

- [1] Alsubari S, Zuhri MYM, Sapuan SM, Ishak MR, Ilyas RA, Asyraf MRM. Potential of natural fiber reinforced polymer composites in sandwich structures: A review on its mechanical properties. *Polymers* 2021; 13: 1-20. <https://doi.org/10.3390/polym13030423>
- [2] Karimah A, Ridho MR, Munawar SS, Adi DS, Damayanti R, Subiyanto B, Fatriasari W, Fudholi A. A review on natural fibers for development of eco-friendly bio-composite: characteristics, and utilizations. *J Mater Res Technol* 2021; 13: 2442-2458. <https://doi.org/10.1016/j.jmrt.2021.06.014>
- [3] Vigneshwaran S, Sundarakannan R, John KM, Joel Johnson RD, Prasath KA, Ajith S, Arumugaprabu V, Uthayakumar M. Recent advancement in the natural fiber polymer composites: A comprehensive review. *J Clean Prod* 2020; 277: 124109. <https://doi.org/10.1016/j.jclepro.2020.124109>
- [4] Asim M, Paridah MT, Chandrasekar M, Shahroze RM, Jawaid M, Nasir M, Siakeng R. Thermal stability of natural fibers and their polymer composites. *Iran Polym J* 2020; 29: 625-648. <https://doi.org/10.1007/s13726-020-00824-6>
- [5] Silva G, Kim S, Aguilar R, Nakamatsu J. Natural fibers as reinforcement additives for geopolymers - A review of potential eco-friendly applications to the construction industry. *Sustain Mater Technol* 2020; 23: e00132. <https://doi.org/10.1016/j.susmat.2019.e00132>
- [6] Jiratti T, Vijay R, Vinod A, Techawinyutham L, Srisuk R, Yorseng K, Sanjay MR, Siengchin S. Lignocellulose sustainable composites from agro-waste Asparagus bean stem fiber for polymer casting applications: Effect of fiber treatment. *Int J Biol Macromol* 2024; 278: 134884. <https://doi.org/10.1016/j.ijbiomac.2024.134884>
- [7] Andrea VL, Panagiota R, Nathalie M, Gérard M, Alain D. Oxidation treatments to convert paper-grade Eucalyptus kraft pulp into micro fibrillated cellulose. *Carbohydr Polym* 2022; 296: 119946. <https://doi.org/10.1016/j.carbpol.2022.119946>
- [8] Brailson Mansingh B, Binoj JS, Quan Z, Eugene WWL, Amornsakchai T, Hassan SA, Kheng LG. Characterization and Performance of Additive Manufactured Novel bio-waste Polylactic acid eco-friendly Composites. *J Polym Environ* 2023; 31: 2306-2320. <https://doi.org/10.1007/s10924-023-02758-5>
- [9] Haradhan K, Kazuharu H, Chun-Won K. Ammonium persulfate treatment on carbohydrate polymers and lignin of wood improved sound absorption capacity. *Int J Biol Macromol* 2022; 205: 626-637. <https://doi.org/10.1016/j.ijbiomac.2022.02.075>
- [10] Manash PM, Shishir S, Vijay P. Optimizing the oxalic acid treatment of cellululosic Himalayan nettle fibre for reinforcement in polymer composites. *Carbohydr Polym* 2022; 296: 119937. <https://doi.org/10.1016/j.carbpol.2022.119937>
- [11] Vijay R, Sathyamoorthy G, Vinod A, Lenin Singaravelu D, Sanjay MR, Siengchin S. Effective utilization of surface-processed/untreated *Cardiospermum halicababum* agro-waste fiber for automobile brake pads and its tribological performance. *Tribol Int* 2024; 197: 109776. <https://doi.org/10.1016/j.triboint.2024.109776>
- [12] Jiratti T, Vinod A, Vijay R, Sanjay MR, Siengchin S. Characterization of novel natural cellulose fiber from *Ficus macrocarpa* bark for lightweight structural composite application and its effect on chemical treatment *Heliyon* 2024; 10(9): e30442. <https://doi.org/10.1016/j.heliyon.2024.e30442>
- [13] Rajeshkumar G, Arvindh Seshadri S, Devnani GL, Sanjay MR, Siengchin S, Prakash Maran J, Al-Dhabi NA, Karuppiah P, Mariadhas VA, Sivarajasekar N, Ronaldo Anuf A. Environment friendly, renewable and sustainable poly lactic acid (PLA) based natural fiber reinforced composites - A comprehensive review. *J Clean Prod* 2021; 310: 127483. <https://doi.org/10.1016/j.jclepro.2021.127483>
- [14] Binoj JS, Jaafar M, Brailson Mansingh B, Bharathiraja G. Extraction and characterization of novel cellulosic biofiber from peduncle of *Areca catechu* L. biowaste for sustainable biocomposites. *Biomass Conv Bioref* 2024; 14: 20359-20367. <https://doi.org/10.1007/s13399-023-04081-4>
- [15] Khalid MY, Al Rashid A, Arif ZU, Ahmed W, Arshad H, Zaidi AA. Natural fiber reinforced composites: Sustainable

- materials for emerging applications. *Results Eng* 2021; 11: 100263.  
<https://doi.org/10.1016/j.rineng.2021.100263>
- [16] Bharath KN, Binoj JS, Brailson Mansingh B, Manjunath GB, Raghu GV, Siengchin S, Sanjay MR. Effect of stacking sequence and interfacial analysis of biomass sheep wool/glass fiber reinforced epoxy biocomposites. *Biomass Conv Bioref* 2024; 14: 17533-17542.  
<https://doi.org/10.1007/s13399-023-03918-2>
- [17] Anne Kavitha S, Krishna Priya R, Krishna Prakash A, Siva A, Maureira-Carsalade N, Roco-Videla A. Investigation on Properties of Raw and Oxalic acid Treated Novel Cellulosic Root Fibres of Zea Mays for Polymeric Composites *Polymers* 2023; 15: 1802-1823.  
<https://doi.org/10.3390/polym15071802>
- [18] Michaela Olisha SL, Emmanuel Victor DB, Julius LL, Jr. Oxalic acid-enzymatic treatment of *Bambusa blumeana* textile fibers for natural fiber-based textile material production. *Ind Crop Prod* 2023; 194: 116268.  
<https://doi.org/10.1016/j.indcrop.2023.116268>
- [19] Maguteeswaran R, Prathap P, Satheeshkumar S, Madhu S. Effect of oxalic acid treatment on novel natural fiber extracted from the stem of *Lankaran acacia* for polymer composite applications. *Biomass Conv Bioref* 2024; 14: 8091-8101.  
<https://doi.org/10.1007/s13399-023-04189-7>
- [20] Vijay R, Vinod A, James Dhillip JD, Sundarajan D, Sanjay MR, Siengchin S. Influence of alkali-treated and raw *Zanthoxylum acanthopodium* fibers on the mechanical, water resistance, and morphological behavior of polymeric composites for lightweight applications. *Biomass Conv Bioref* 2024; 14: 24345-24357.  
<https://doi.org/10.1007/s13399-023-04240-7>
- [21] Juvvi SNR, Melvin VD, Kumaran P. Comprehensive characterization of raw and oxalic acid ( $C_2H_2O_4$ ) treated natural fibers from *Symphirema involucratum* stem. *Int J Biol Macromol* 2021; 186: 886-896.  
<https://doi.org/10.1016/j.ijbiomac.2021.07.061>
- [22] Baskara Sethupathi P, Sundaram M, Palani V, Vijay R, James Dhillip JD, Anish K. Characterization of silane treated and untreated *Citrullus lanatus* fibers based eco-friendly automotive brake friction composites. *J Nat Fibers* 2022; 19(16): 13273-13287.  
<https://doi.org/10.1080/15440478.2022.2089431>
- [23] Vijay R, Sathyamoorthy G, Vinod A, Lenin Singaravelu D, Sanjay MR, Siengchin S. Sustainable characterization of brake pads using raw/silane-treated *Mimosa pudica* fibers for automobile applications. *Polym Compos* 2024; 45(11): 10204-10219.  
<https://doi.org/10.1002/pc.28467>
- [24] Li M, Pu Y, Thomas VM, Yoo CG, Ozcan S, Deng Y, Nelson K, Ragauskas AJ. Recent advancements of plant-based natural fiber-reinforced composites and their applications. *Compos B Eng* 2020; 200: 108254.  
<https://doi.org/10.1016/j.compositesb.2020.108254>
- [25] Hariharan G, Krishnamachary PC, Binoj JS, Brailson Mansingh B. Influence of SiC Nanoparticles Reinforcement in *Areca/Tamarind Hybrid Biopolymer Composites*: Thermo-mechanical, Tribological and Morphological Features. *J Bionic Eng* 2023; 20: 1723-1736.  
<https://doi.org/10.1007/s42235-023-00341-1>
- [26] Binoj JS, Jaafar M, Brailson Mansingh B, Koya Pulikkal A. Comprehensive investigation of *Areca catechu* tree peduncle biofiber reinforced biocomposites: influence of fiber loading and surface modification. *Biomass Conv Bioref* 2024; 14: 23001-23013.  
<https://doi.org/10.1007/s13399-023-04182-0>
- [27] Brailson Mansingh B, Binoj JS, Minther Singh AAM, Francis Britto AS. Influence of SiC nanoparticles on properties of alkali-treated areca fruit husk fiber/hybrid polymer composites. *J Appl Polym Sci* 2023; 140(10): e53591.  
<https://doi.org/10.1002/app.53591>
- [28] Saikrishnan G, Yoganjaneyulu G, Jegan Mohan SR, Vijay R, James Dhillip JD. Influence of stacking sequence on the mechanical and water absorption characteristics of areca sheath-palm leaf sheath fibers reinforced epoxy composites *J Nat Fibers* 2022; 19(5): 1670-1680.  
<https://doi.org/10.1080/15440478.2020.1787921>
- [29] Hanan UA, Hassan SA, Wahit MU, Binoj JS, Brailson Mansingh B, Kheng LG. Experimentation, optimization, and predictive analysis of compressive behavior of montmorillonite nano-clay/unsaturated polyester composites. *Polym Compos* 2023; 44: 241-251.  
<https://doi.org/10.1002/pc.27041>
- [30] Anish K, Vijay R, Lenin Singaravelu D, Sanjay MR, Siengchin S, Jawaid M, Alamry KA, Asiri AM. Extraction and characterization of cellulose fibers from the stem of *momordica charantia*. *J Nat Fibers* 2022; 19(6): 2232-2242.  
<https://doi.org/10.1080/15440478.2020.1807442>
- [31] Keya KN, Kona NA, Koly FA, Maraz KM, Islam MN, Khan RA. Natural fiber reinforced polymer composites: history, types, advantages, and applications. *Mater Eng Res* 2019; 1: 69-87.  
<https://doi.org/10.25082/mer.2019.02.006>
- [32] Balla VK, Kate KH, Satyavolu J, Singh P, Tadimetri JGD. Additive manufacturing of natural fiber reinforced polymer composites: Processing and prospects. *Compos B Eng* 2019; 174: 106956.  
<https://doi.org/10.1016/j.compositesb.2019.106956>
- [33] Mazzanti V, Pariante R, Bonanno A, Ruiz de Ballesteros O, Mollica F, Filippone G. Reinforcing mechanisms of natural fibers in green composites: Role of fibers morphology in a PLA/hemp model system. *Compos Sci Technol* 2019; 180: 51-59.  
<https://doi.org/10.1016/j.compscitech.2019.05.015>
- [34] Sarikaya E, Çallioğlu H, Demirel H. Production of epoxy composites reinforced by different natural fibers and their mechanical properties. *Compos B Eng* 2019; 167: 461-466.  
<https://doi.org/10.1016/j.compositesb.2019.03.020>
- [35] Dao C, Beibei W, Yuxia C, Shengcheng Z, Chenxin W, Runmin X, Junkui G, Yan L, Lanlan S, Yong G. Characterization of potential cellulose performance of *Luffa* vine: A study on physicochemical and structural properties *Int J Biol Macromol* 2020; 164: 2247-2257.  
<https://doi.org/10.1016/j.ijbiomac.2020.08.098>
- [36] Vijay R, James Dhillip JD, Gowtham S, Harikrishnan SBMA, Chandru B, Amarnath M, Anish K. Characterization of natural cellulose fiber from the barks of *vachellia farnesiana*. *J Nat Fibers* 2022; 19(4): 1343-1352.  
<https://doi.org/10.1080/15440478.2020.1764457>
- [37] Brailson Mansingh B, Binoj JS, Abu Hassan S, Eugene Wong WL, Suryanto H, Shengjie L, Lim Goh K. Feasibility study on thermo-mechanical performance of 3D printed and annealed coir fiber powder/poly(lactic acid) eco-friendly biocomposites. *Polym Compos* 2024; 45(7): 6512-6524.  
<https://doi.org/10.1002/pc.28214>
- [38] Francis Britto AS, Rajesh Prabha N, Brailson Mansingh B, David R, Minther Singh AAM, Binoj JS. Extraction and characterization of *Dypsis lutescens* peduncle fiber: agro-waste to probable reinforcement in biocomposites—a sustainable approach. *Biomass Conv Bioref* 2025; 15: 2275-2284.  
<https://doi.org/10.1007/s13399-023-04950-y>
- [39] Brailson Mansingh B, Binoj JS, Siengchin S, Sanjay MR. Influence of surface treatment on properties of *Cocos nucifera* L. *Var typica* fiber reinforced polymer composites. *J Appl Polym Sci* 2023; 140: e53345.  
<https://doi.org/10.1002/app.53345>
- [40] Wenbin X, Hanpeng W, Wei W, Fubin H, Zihan B. Macro-Micro Damage and Failure Behavior of Creep Gas-Bearing Coal Subjected to Drop Hammer Impact. *Nat Resour Res* 2024; 33: 707-725.  
<https://doi.org/10.1007/s11053-023-10302-4>

- [41] Ji D, Zhao H, Vanapalli SK. Damage evolution and failure mechanism of coal sample induced by impact loading under different constraints. *Nat Resour Res* 2023; 32: 619-647. <https://doi.org/10.1007/s11053-022-10156-2>
- [42] Thooyavan Y, Kumaraswamidhas LA, Edwin Raj RD, Binoj JS, Brailson Mansingh B, Francis Britto AS, Alamry A. Modelling and Characterization of Basalt/Vinyl Ester/SiC Micro- and Nano-hybrid Biocomposites Properties Using Novel ANN-GA Approach. *J Bionic Eng* 2024; 21: 938-952. <https://doi.org/10.1007/s42235-024-00482-x>
- [43] Merve ST, Emine O, Hüseyin I, Emircan O, Hüseyin U, Mustafa Ş. Characterization of chemically treated waste wood fiber and its potential application in cementitious composites. *Cem Concr Compos* 2023; 137: 104938. <https://doi.org/10.1016/j.cemconcomp.2023.104938>
- [44] Samant L, Alka G, Jessen M, Seiko J, Sabu T. Effect of surface treatment on flax fiber reinforced natural rubber green composite. *J Appl Polym Sci* 2023; 140: e53651. <https://doi.org/10.1002/app.53651>
- [45] Shanmugasundaram N, Rajendran I, Ramkumar T. Characterization of untreated and oxalic acid treated new cellulosic fiber from an Areca palm leaf stalk as potential reinforcement in polymer composites. *Carbohydr Polym* 2018; 195: 566-575. <https://doi.org/10.1016/j.carbpol.2018.04.127>
- [46] Jaya Sheeba KR, Jagadeesh KA, Jeyaprakash D, Anne KS, Sutha S, Sundaram A, Manoharan V, Moonyong L, Krishna Priya R. Physico-chemical and extraction properties on oxalic acid-treated *Acacia pennata* fiber. *Environ Res* 2023; 233: 116415. <https://doi.org/10.1016/j.envres.2023.116415>
- [47] Tamil Moli L, Mohamed Thariq HS, Qumrul A, Mohammad J, Jesuarockiam N, Md Ain Umaira S, Lee Seng H. Characterization of oxalic acid treated new cellulosic fibre from *Cyrtostachys renda*. *J Mater Res Technol* 2020; 9: 3537-3546. <https://doi.org/10.1016/j.jmrt.2020.01.091>
- [48] Ganapathy T, Senthamaraiannan P, Murugeswari K, Arivazhagan S, Santhoshkumar M. Suitability Evaluation of Raw and Oxalic acid-Treated Cannonball Fibers as Reinforcement in Polymer Composites. *Waste Biomass Valorization* 2024; 15: 5125-5136. <https://doi.org/10.1007/s12649-024-02514-3>
- [49] Ganapathy T, Sathiskumar R, Senthamaraiannan P, Saravanakumar SS, Anish K. Characterization of raw and oxalic acid treated new natural cellulosic fibres extracted from the aerial roots of banyan tree. *Int J Biol Macromol* 2019; 138: 573-581. <https://doi.org/10.1016/j.ijbiomac.2019.07.136>
- [50] Beschi Selvan SL, Francis Britto AS, Brailson Mansingh B, Binoj JS. Extensive characterization of optimally treated *Licuala grandis* leaf sheath fiber for possible bio-reinforcement in polymer composites. *J Appl Polym Sci* 2024; 141(45): e56195. <https://doi.org/10.1002/app.56195>
- [51] Ponnusamy DA, Gajendiran H, Brailson Mansingh B, Binoj JS. Diffractonal, spectroscopical, morphological, and thermal analysis of pretreated/enzyme modified cellulosic *Cocos nucifera* L. peduncle fiber. *Biomass Conv Bioref* 2025; 15: 3115-3126. <https://doi.org/10.1007/s13399-023-05076-x>
- [52] Rathinavelu R, Paramathma BS. Examination of characteristic features of raw and oxalic acid-treated cellulosic plant fibers from *Ventilago maderaspatana* for composite reinforcement. *Biomass Conv Bioref* 2023; 13: 4413-4425. <https://doi.org/10.1007/s13399-022-03461-6>
- [53] Vijay R, Kumaran P, Pottathil S, James Dhilip JD, Yoganjaneyulu G, Saikrishnan G. Influence of *Parthenium hysterophorus* and *Impomea pes-caprae* fibers stacking sequence on the performance characteristics of epoxy composites. *J Nat Fibers* 2022; 19(12): 4456-4466. <https://doi.org/10.1080/15440478.2020.1863292>
- [54] Manivel MV, Natrayan L, Kaliappan S, Pravin PP. Grape stalk cellulose toughened plain weaved bamboo fiber-reinforced epoxy composite: load bearing and time-dependent behavior. *Biomass Conv Bioref* 2024; 14: 14317-14324. <https://doi.org/10.1007/s13399-022-03702-8>
- [55] Venugopal A, Boominathan SK. Physico-chemical, thermal and tensile properties of oxalic acid-treated *Acacia concinna* fiber. *J Nat Fibers* 2022; 19: 3093-3108. <https://doi.org/10.1080/15440478.2020.1838998>
- [56] Cornelia HH, Serna-Loaiza S, Irmgard W, Luisa S, Ayse Nur K, Zelaya-Lainez L, Josef F, Hinrich G, Ulrich H, Anton F, Michael H. Comparison of coupled chemical pretreatment and mechanical refining of spruce sawdust: fiber network properties and initial production of lignin-bonded biocomposites. *Biomass Conv Bioref* 2024; 14: 15469-15482. <https://doi.org/10.1007/s13399-023-03796-8>
- [57] Binoj JS, Jaafar M, Brailson Mansingh B, Raghu R. Viscoelastic and heat-resistant behavior of surface-treated areca fruit husk fiber-reinforced polymer composites. *Iran Polym J* 2023; 32: 841-853. <https://doi.org/10.1007/s13726-023-01169-6>
- [58] Senthamaraiannan P, Saravanakumar SS. Effect of *Cocos nucifera* shell powder on mechanical and thermal properties of *Mucuna atropurpurea* stem fibre-reinforced polyester composites. *Biomass Conv Bioref* 2023; 13: 11275-11294. <https://doi.org/10.1007/s13399-022-03621-8>
- [59] Baskaran PG, Kathiresan M, Pandiarajan P. Effect of oxalic acid-treatment on structural, thermal, tensile properties of *Dichrostachys cinerea* bark fiber and its composites. *J Nat Fibers* 2022; 19: 433-449. <https://doi.org/10.1080/15440478.2020.1745123>
- [60] Syafri E, Jamaluddin, Nasmi Herlina S, Melbi M, Putri A, Rushdan AI. Isolation and characterization of cellulose nanofibers from *Agave gigantea* by chemical-mechanical treatment. *Int J Biol Macromol* 2022; 200: 25-33. <https://doi.org/10.1016/j.ijbiomac.2021.12.111>
- [61] Prithiviraj M, Muralikannan R. Investigation of optimal oxalic acid-treated *perotis indica* plant fibers on physical, chemical, and morphological properties. *J Nat Fibers* 2022; 19: 2730-2743. <https://doi.org/10.1080/15440478.2020.1821291>
- [62] Fan L, Tianxuan H, Guoqing W, Yiju T, Meiqi Y, Lizhen Z. Mechanical Properties and Fractal Characteristics of Fractured Coal Under Different Gas Pressures. *Nat Resour Res* 2024; 33: 793-812. <https://doi.org/10.1007/s11053-023-10305-1>
- [63] Palai BK, Sarangi SK. Characterization of untreated and oxalic acidized *Eichhornia crassipes* fibers and its composites. *J Nat Fibers* 2020; 19: 3809-3824. <https://doi.org/10.1080/15440478.2020.1848729>
- [64] Hendri H, Jamasri, Kusmono. A Preliminary Study: Influence of Oxalic acid Treatment on Physical and Mechanical Properties of *Agel* Leaf Fiber (*Corypha gebanga*). *Appl Mech Mat* 2016; 842: 61-66. <https://doi.org/10.4028/www.scientific.net/AMM.842.61>
- [65] Yao Q, Zheng C, Shang X, Yan L, Shan C, Wang W. Evolution of mechanical and acoustic emission characteristics of coal samples under different immersion heights. *Nat Resour Res* 2023; 32: 2273-2288. <https://doi.org/10.1007/s11053-023-10242-z>
- [66] Yuges MT, Saroj KS. Characterization of raw and oxalic acid treated cellulosic *Grewia Flavescens* natural fiber. *Int J Biol Macromol* 2022; 209: 1933-1942. <https://doi.org/10.1016/j.ijbiomac.2022.04.169>

- [67] Maria G, Pereira-Rojas J, Villanueva I, Agüero B, Iris S, Ingrid V, Blass D, Javier H, Gleen R, Henry L, Haydn B, Juan P. Preparation and characterization of cellulose fibers from *Meghatyrus maximus*: Applications in its chemical derivatives. *Carbohydr Polym* 2022; 296: 119918. <https://doi.org/10.1016/j.carbpol.2022.119918>
- [68] Vijay R, Jafrey DJD, Gowtham S, Harikrishnan S, Chandru B, Amarnath M, Anish K. Characterization of natural cellulose fiber from the barks of *Vachellia farnesiana*. *J Nat Fibers* 2022; 19: 1343-1352. <https://doi.org/10.1080/15440478.2020.1764457>
- [69] Sabarinathan P, Rajkumar K, Annamalai VE, Vishal K. Characterization on chemical and mechanical properties of silane treated fish tail palm fibres. *Int J Biol Macromol* 2020; 163: 2457-2464. <https://doi.org/10.1016/j.ijbiomac.2020.09.159>
- [70] Umashankaran M, Gopalakrishnan S. Effect of sodium hydroxide treatment on physico-chemical, thermal, tensile and surface morphological properties of *Pongamia Pinnata* L. bark fiber. *J Nat Fibers* 2021; 18: 2063-2076. <https://doi.org/10.1080/15440478.2019.1711287>
- [71] Li HQ, Feng ZJ, Zhang CP. Characterization of coal pore structure and matrix compressibility by water vapor injection. *Nat Resour Res* 2022; 31(5): 2869-2883. <https://doi.org/10.1007/s11053-022-10109-9>
- [72] Arul MMA, Ravindran D, Sundara Bharathi SR, Indran S, Suganya Priyadarshini G. Characterization of surface-modified natural cellulosic fiber extracted from the root of *Ficus religiosa* tree. *Int J Biol Macromol* 2020; 156: 997-1006. <https://doi.org/10.1016/j.ijbiomac.2020.04.117>
- [73] Linhu D, Xiaoshuai H, Lihua C, Yiming C, Zhe L, Jingquan H, Shuijian H, Shaohua J. Characterization of natural fiber from manau rattan (*Calamus manan*) as a potential reinforcement for polymer-based composites. *J Bioresour* 2022; 7: 190-200. <https://doi.org/10.1016/j.jobab.2021.11.002>
- [74] Changhao S, Qiangling Y, Shenggen C, Qiang X, Chuangkai Z, Ze X, Yinghu L, Lun Y. Fracture development Patterns and Micro-Macrostructural Fractal Characteristics of Acid-Base Coal Samples. *Nat Resour Res* 2024; 33: 831-865. <https://doi.org/10.1007/s11053-024-10313-9>

Received on 12-04-2025

Accepted on 10-05-2025

Published on 09-06-2025

<https://doi.org/10.6000/1929-5995.2025.14.04>© 2025 Arabilachi *et al.*

This is an open-access article licensed under the terms of the Creative Commons Attribution License (<http://creativecommons.org/licenses/by/4.0/>), which permits unrestricted use, distribution, and reproduction in any medium, provided the work is properly cited.